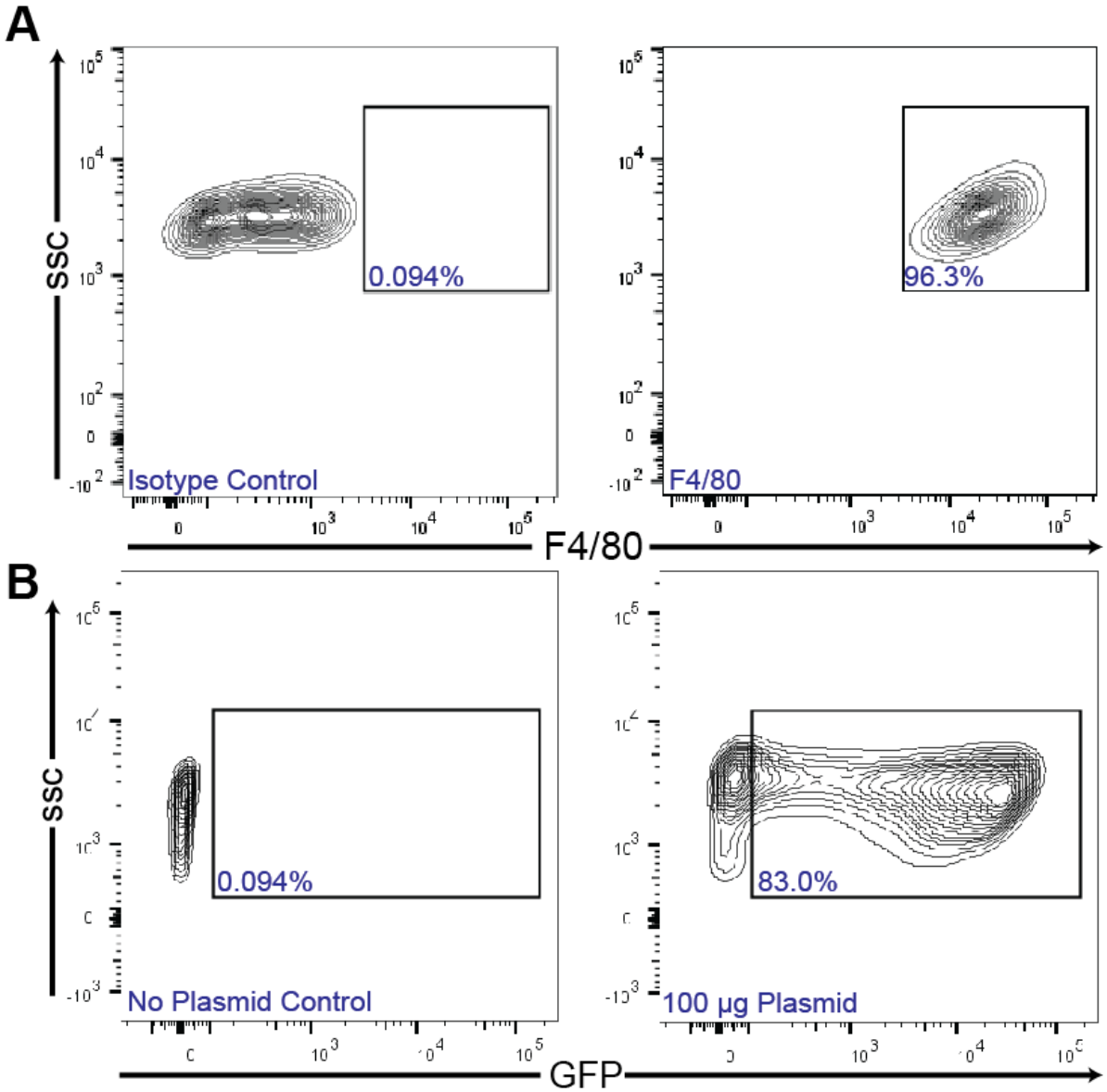

Supplementary Figure S1. Bone marrow-derived monocyte purity and electroporation efficiency
(A) Harvested BMDMs exhibited 96.3% purity by F4/80 staining after 5 days of differentiation in 20 ng/mL murine macrophage colony stimulating factor. **(B)** BMDMs were electroporated with the pARG1-Gluc reporter plasmid with an efficiency of >80% and viability ~60% as quantified by flow cytometry.

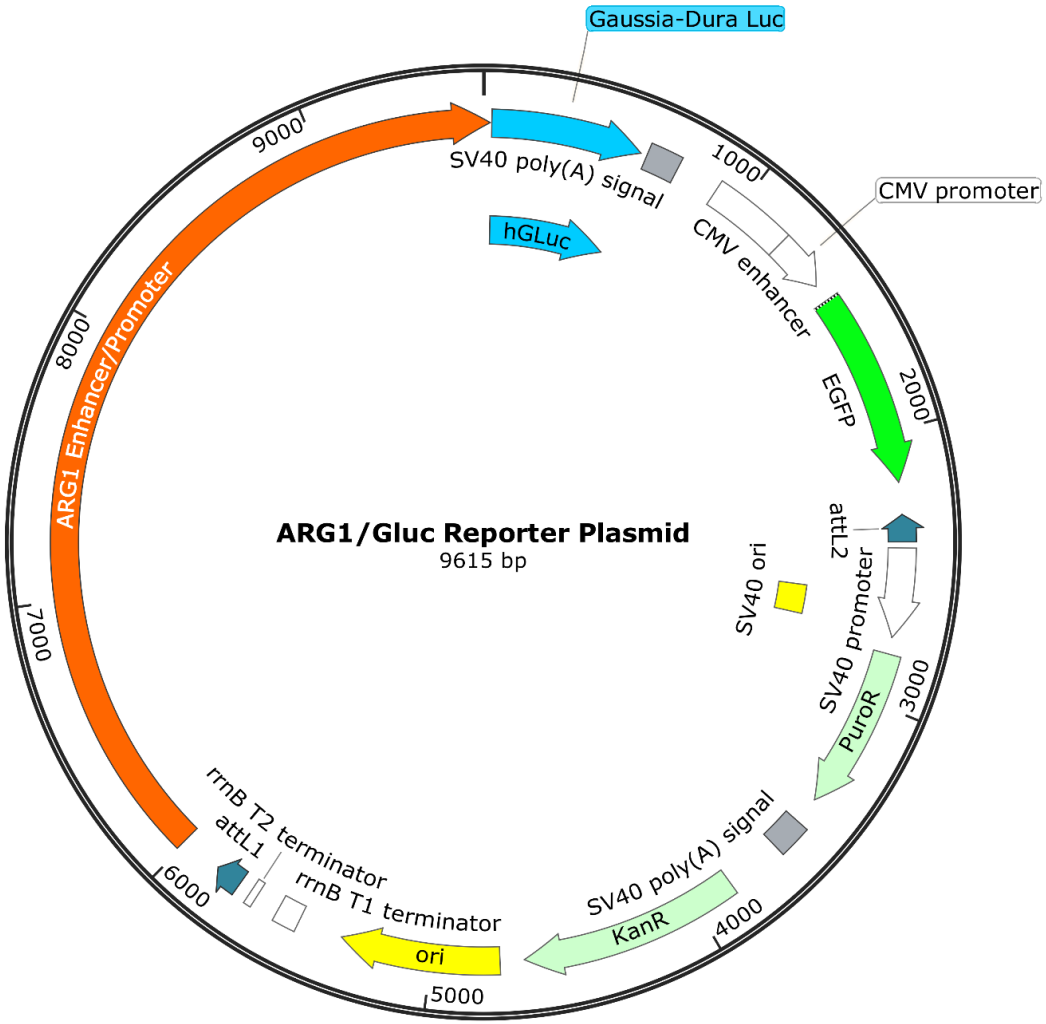

Supplementary Figure S2. pARG1-Gluc reporter plasmid map
The pARG1-Gluc construct contains the *Gaussia* Dura Luciferase immediately downstream of the 3780 base pair ARG1 enhancer/promoter sequence. The construct also contains the gene for eGFP under the control of the constitutive CMV promoter for cell sorting and determining transfection efficiency.

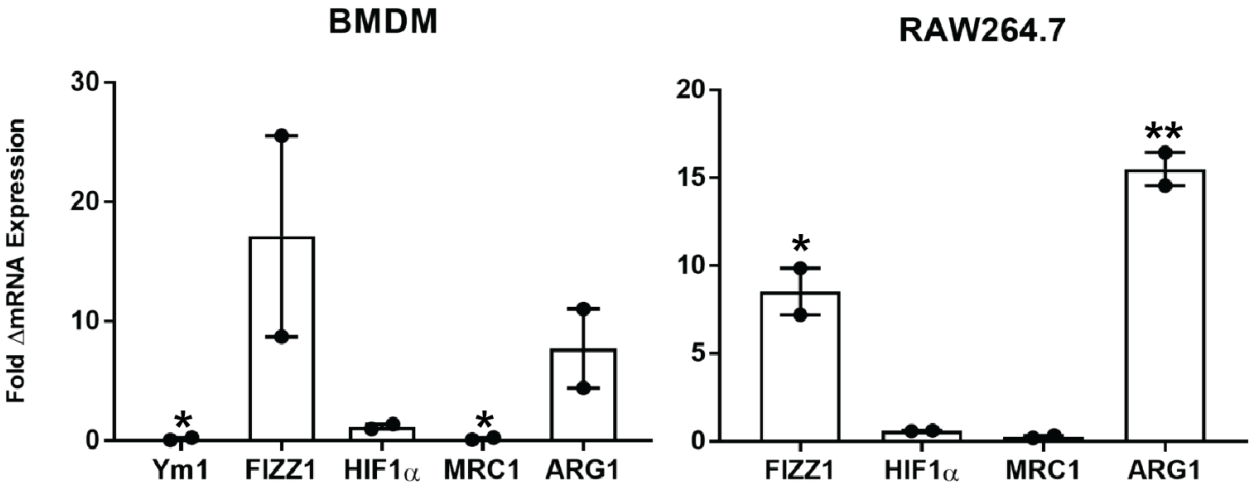

Supplementary Figure S3. Lactic acid induces ARG1 expression in macrophages.
100 mM Lactic acid induces expression of FIZZ1 and ARG1 mRNA in both bone marrow derived (left) and RAW264.7 (right) macrophages 24 hours after stimulation. * indicates statistical significance at $p < 0.05$, ** indicates statistical significance at $p < 0.01$. Error bars depict standard error of the mean. BMDM, bone marrow-derived macrophage.

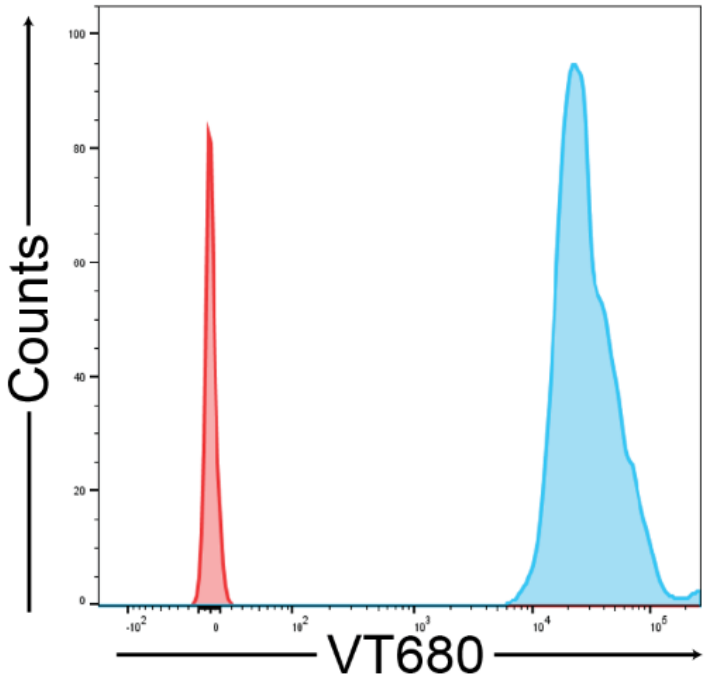

Supplementary Figure S4. VivoTrack 680 labeling of RAW264.7 macrophages
Uniform labeling of macrophages (blue) was observed with 4-5 orders of magnitude of fluorescence above unstained macrophages (red).

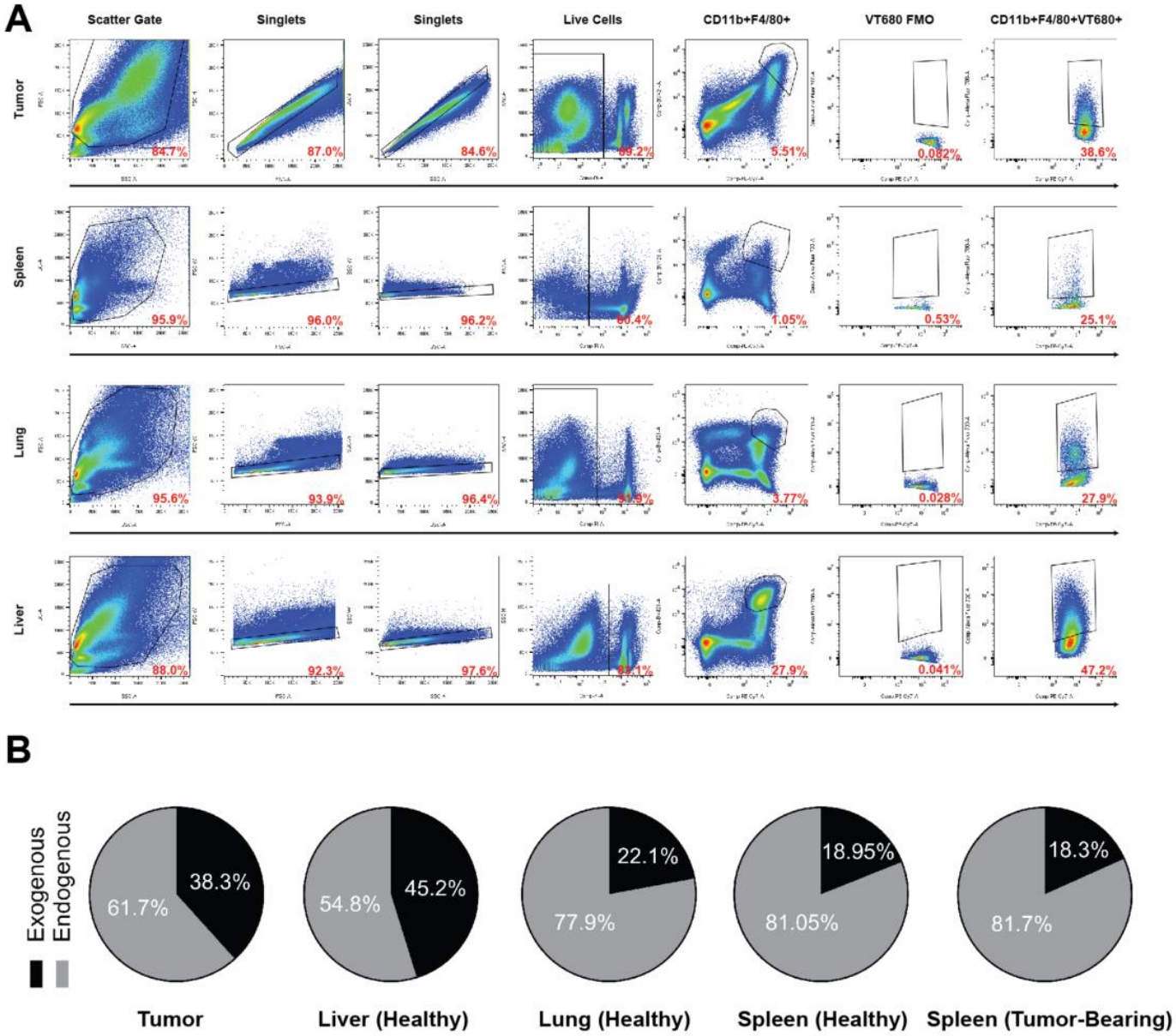

Supplementary Figure S5. Flow cytometry gating strategy for macrophage sorting
(A) Flow cytometry gating strategy for adoptively transferred (VT680+) and native (VT680-) macrophages in tumor, spleen, lung, and liver. Populations for CD11b+F4/80+ cells were well-separated in both tissues and adoptively transferred macrophages were gated based on a fluorescence minus one control. FMO, fluorescence minus one. **(B)** Average fractional makeup of administered (VT680+) vs. endogenous (VT680-) macrophages present in various tissues five days after adoptive transfer.

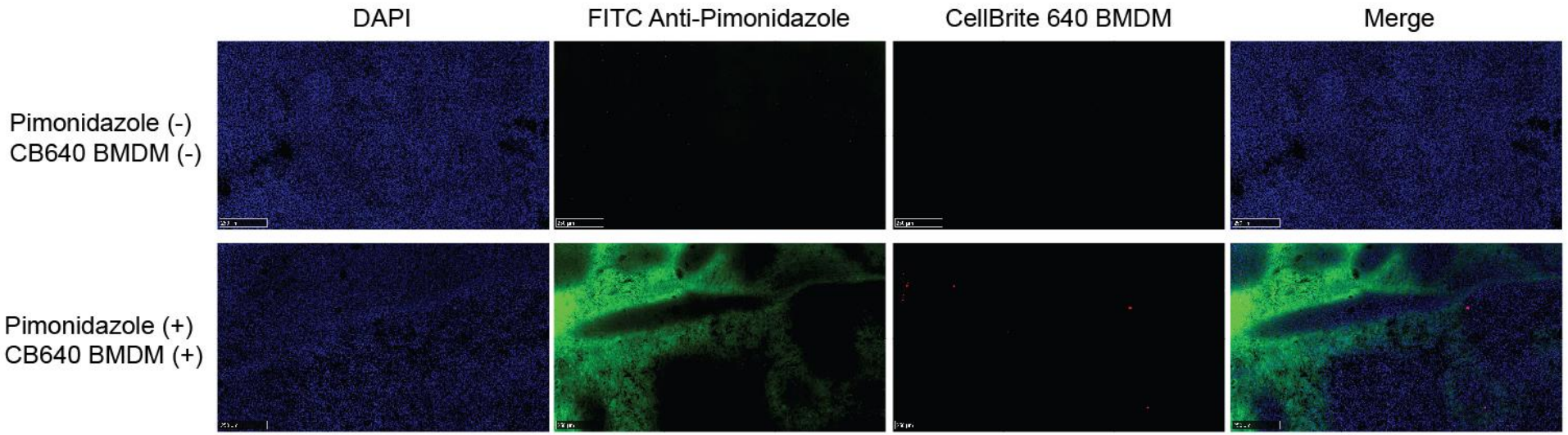

Supplementary Figure S6. Immunofluorescence of macrophage localization relative to hypoxia in CT26 tumors
Immunofluorescence of CT26 tumors from mice injected with fluorescently labeled bone marrow derived monocytes (bottom) reveals co-localization of macrophages (red) with regions of hypoxia (green). Immunofluorescence of a CT26 tumor from mice not injected with pimonidazole and injected with non-fluorescently labeled bone marrow derived monocytes (top) does not show any signal in the green or red channels confirming specificity. Images are shown at 10x magnification and scale bars measure 250 μm. CB640, CellBrite 640; BMDM, bone marrow derived monocytes.

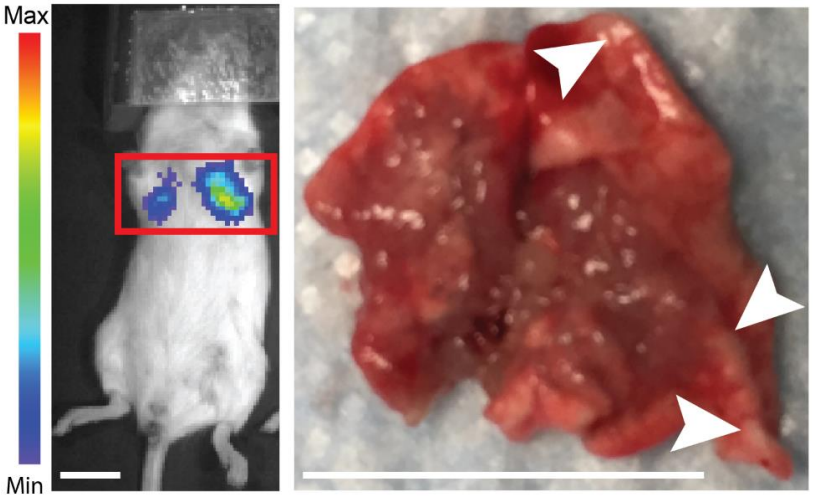

Supplementary Figure S7. Lung microtumors in a model of metastatic breast cancer
One week after intravenous injection of 4T1 cells, disease burden remains localized to the lungs as visualized by BLI (left). *Ex vivo* examination of the lungs also reveals non-elevated microtumors lining the lung pleura (right). Scale bars measure 1 cm.

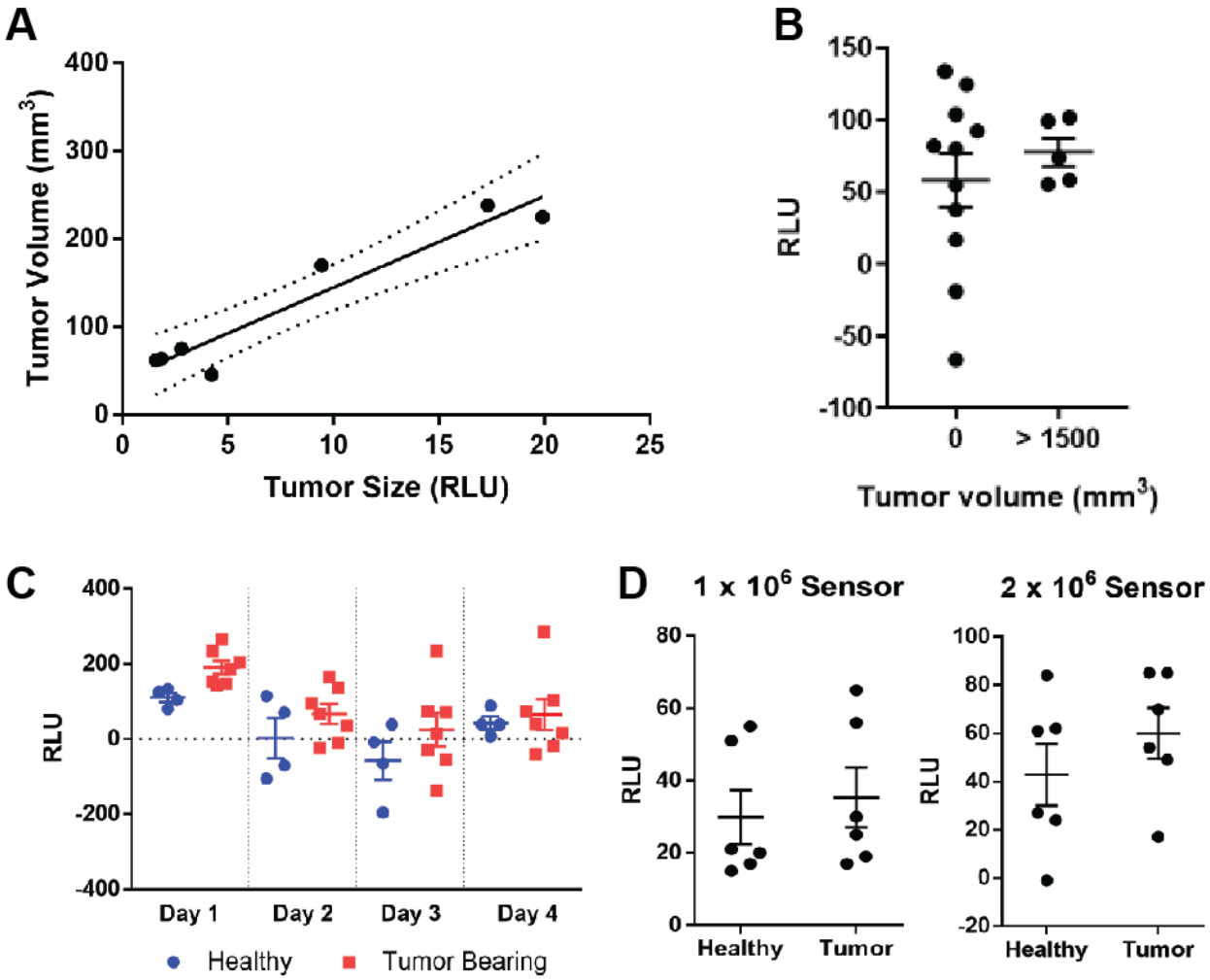

Supplementary Figure S8. Macrophage sensor optimization in subcutaneous localized model of colorectal cancer
(A) Tumor volumes measured by digital caliper are well-correlated with tumor volumes estimated by BLI (r^2 = 0.918). Dashed lines show 95% confidence interval of the linear regression. **(B)** The engineered macrophage sensor was unable to detect visibly necrotic tumors with volumes > 1500 mm^3, possibly due to poor infiltration of the sensor due into the avascular tumor cores. **(C)** In detection of 50-250 mm^3 localized subcutaneous tumors, elevated plasma Gluc compared to healthy controls was apparent 24 hours after macrophage sensor injection but signal declined in subsequent days in both healthy and tumor bearing mice. **(D)** In the same tumor model, 1 million and 2 million injected macrophage sensors were unable to reliably distinguish tumor bearing mice from healthy controls. Refer to the main text for results with 3 million injected macrophage sensors. Error bars depict standard error of the mean. RLU, relative luminescence units.

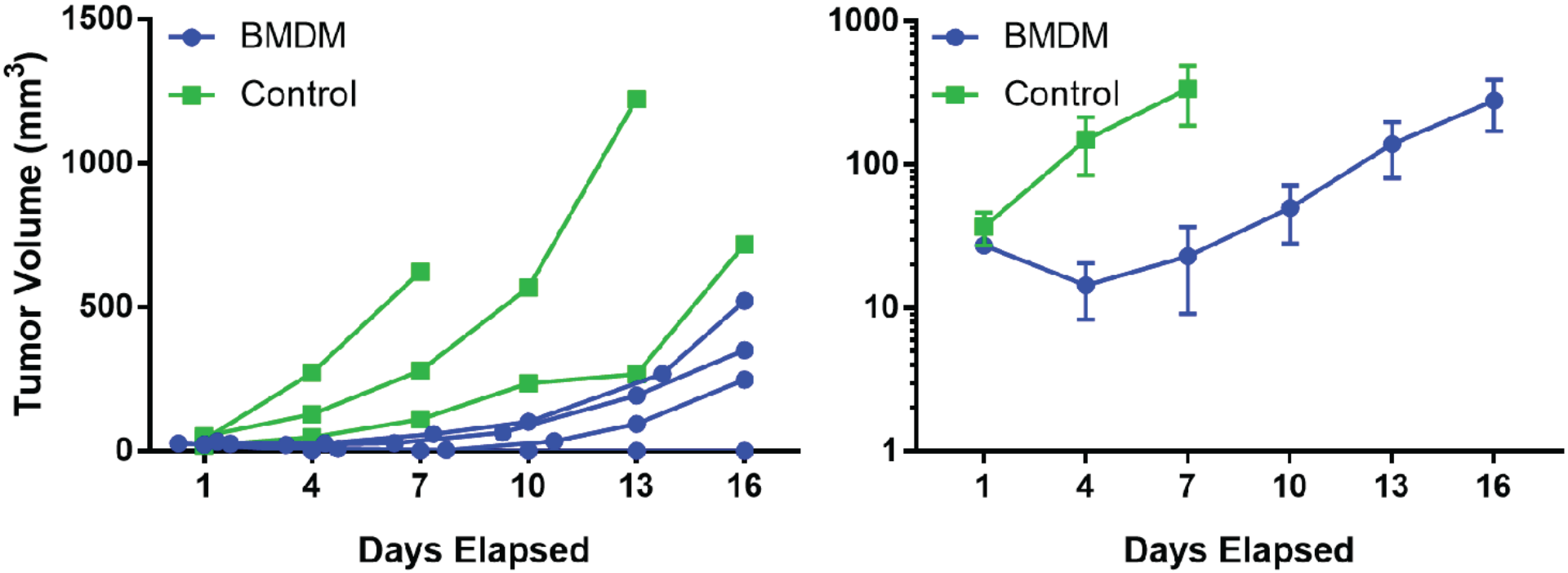

Supplementary Figure S9. The effect of intravenously injected macrophage sensor on tumor progression.
(A) Intravenous injection of BMDM sensor in subcutaneous tumor-bearing mice (n = 4) leads to an initial regression (Day 4, p = 0.058) of tumor volume relative to vehicle injected mice (n = 3) followed by resumption of exponential growth. Left plot shows growth of individual tumors and right plot shows average tumor volumes. Mice were sacrificed upon tumors exceeding 15 mm in any dimension and average tumor volumes in right plot are only shown for time points in which all mice in a group were still alive. Error bars depict standard error of the mean. BMDM, bone marrow derived macrophage.

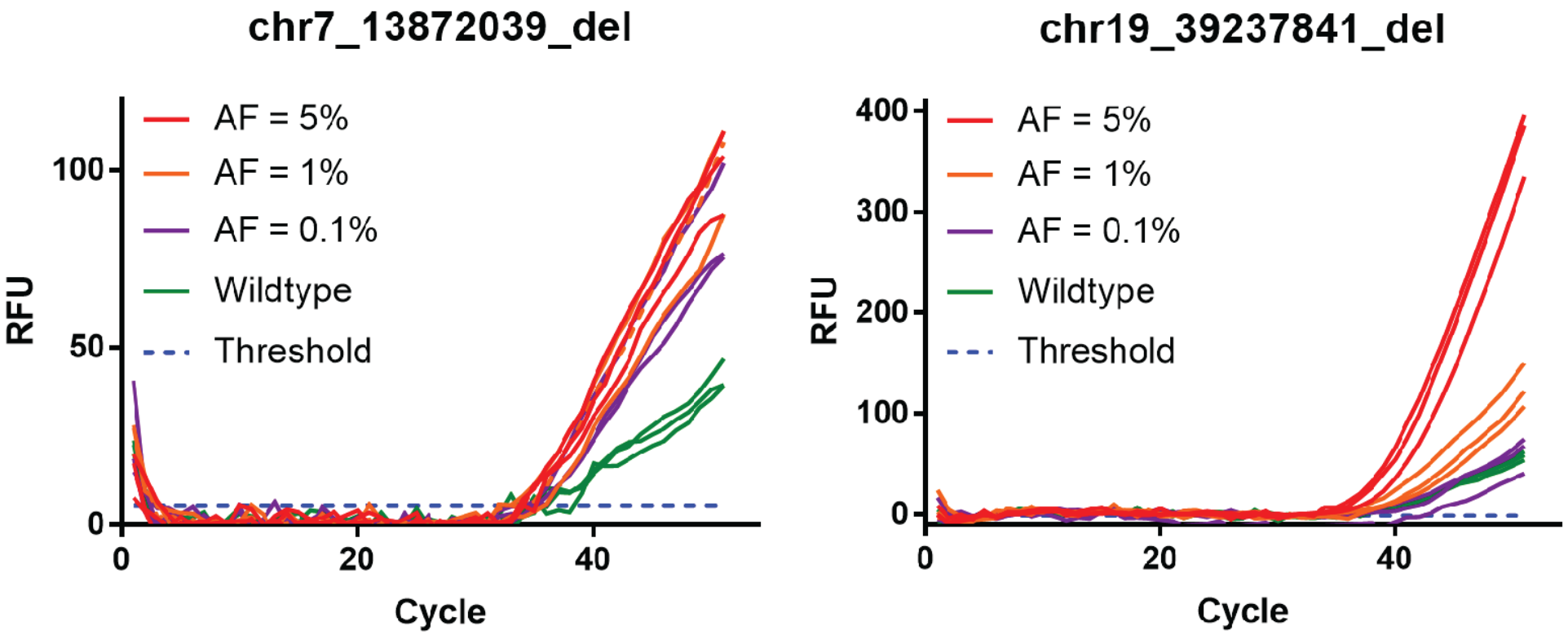

Supplementary Figure S10. Deletion mutation limit of detection with locked nucleic acid probes.
Real-time qPCR amplification plots of CT26 and wildtype Balb/c genomic DNA show that the chromosome 7 (left) and 19 (right) deletions can be detected at allele frequencies of 0.1% and 1% respectively. Each condition is shown in triplicate. RFU, relative fluorescence units; AF, allele frequency.